Chinese Journal of Polar Science, Vol 18, No 1, 54-62, June 2007

Detecting Arctic snow and ice cover with FY-1D global data

Xie Xiaoping(谢小萍)[1], Liu yujie(刘玉洁)[2] and Du bingyu(杜丙玉)[1]

1. School of Remote Sensing of NUIST, Nanjing 210044, China
2. National Satellite Meteorological Center, Beijing 100081, China

Received June 8, 2007

Abstract Chinese meteorological satellite FY-1D can obtain global data from four spectral channels which include visible channel (0.58-0.68 μm) and infrared channels (0.84-0.89 μm, 10.3-11.3 μm, 11.5-12.5 μm). 2366 snow and ice samples, 2024 cloud samples, 1602 land samples and 1648 water samples were selected randomly from Arctic imageries. Land and water can be detected by spectral features. Snow-ice and cloud can be classified by textural features. The classifier is Bayes classifier. By synthesizing five days classifying result of Arctic snow and ice cover area, complete Arctic snow and ice cover area can be obtained. The result agrees with NOAA/NESDIS MS products up to 70%.

Key words FY-1D, Arctic, snow and ice cover, Bayes classification

1 Introduction

The Antarctic and Arctic are key research areas to World Climate Research Programme (WCRP) and International Geosphere-Biosphere Program[1], and attached importance on seriously in previous IPCC reports[2,3]. Detecting Arctic snow and ice cover by satellites is very urgent and important to know the process of climate change and monitoring global warming[4]. According to the the published report of American National Snow and Ice Data Center in September 28th, 2005, for the period 1979 through 2001, before the recent series of low extents, the rate of September Arctic snow and ice cover decline was slightly more than 6.5 percent per decade. After the September 2002 minimum, which was the record before this year, the trend steepened to 7.3 percent. Incorporating the 2005 minimum, with a projection for ice growth in the last few days of September, the estimated decline in end-of-summer Arctic sea ice is now approximately 8 percent per decade. If current rates of decline in sea ice continue, the summertime Arctic could be completely ice-free well before the end of this century. Snow and ice cover in polar area is an important factor by which surface physical process influences climate system, and its seasonal and annual change is not only restricted by but also having great influence on climate system. Keeping a close attention on Arctic snow and ice cover has great significance to both global climate change and China weather and climate.

Currently, it is usually using optical, passive and active radar satellite remote sensing sensors to detecting arctic snow and ice, and sensors of different kinds has their advantages

and disadvantages. Advanced Very High Resolution Radiometer (AVHRR), loaded on NOAA series satellites, whose resolution is 1.1km, can be used to accurately estimate sea ice boundary, sea ice intensity, surface type and temperature[5-7], but its shortcoming is that motionless clouds and long-time night disturb its data acquisition. Clouds and night can not influence passive microwave sensors[8-12]. Special Sensor Microwave/Imager (SSM/I) loaded on Defense Meteorological Satellite Program (DMSP), a multi-channel microwave radiometer, can obtain daily global sea ice intensity data and differentiate multi-year ice and one-year ice[13, 14], but its resolution is low (about 25 km). SAR (Synthetic Aperture Radar) loaded on satellite can detect snow and ice and free of the influence of clouds and night, and its data resolution is very high (about 20 m), so its data is frequently used in the research of snow and ice[15, 16]. Its shortcoming is limited detecting area and cannot be used to global or hemisphere detection.

Since FY-1C/D being launched, China has its own global satellite remote sensing data. FY-1C and 1D have the same sensors-Multichannel Visible and Infrared Scan Radiometer (MVISR), which can obtain global data of visible, near-infrared, and infrared split window channels whose wavelength and data format is similar to that of the 1, 2, 3, 4, 5 channels of NOAA-AVHRR[17]. Up to now, 6 years global data have been collected from the MVISR, and these data is useful to polar snow and ice research. However, because of the lack of NOAA-AVHRR's third channel (1.6 μm in daylight, and 3.7 μm in night) that is effective to distinguish clouds and snow[18-20] previous methods cannot be used for utilizing the data. In this paper, a new method is presented to obtain Arctic snow and ice cover by using the MVISR data.

Based on many test and samples analysis, the difference of the spectral features and texture features between clouds and snow-ice in the four channels of MVISR was understood, and then a discriminant function to distinguish clouds and snow-ice was built. The result is that it is effective to discriminate clouds and snow-ice by spectral feature and texture feature.

2 Data

FY-1D global data (GDPT) are obtained from China National Satellite Meteorological Center. The footprint resolution is 3245 m[21]. There are four channels: channel 1 (0.58-0.68 μm, channel 2 (0.84-0.89 μm), channel 3 (10.3-11.3 μm), channel 4 (11.5-12.5 μm). Because a visible channel was used and the Arctic is in the polar night during winter, the summer data (May-July, 2004-2005) were selected.

3 Feature analysis

According to the experience of satellite meteorologists, various samples, including 2172 snow and ice samples, 2133 clouds samples, 1602 land samples, 1648 water samples, were obtained.

3.1 Spectral feature analysis

It is difficult to distinguish snow and ice from clouds, because the reflectivity f clouds, snow and ice are all high in visible band. In infrared band, the brightness temperature of clouds has a wide range. The brightness temperature of some clouds is lower than snow and ice, and the brightness temperature of some clouds is close to that of snow and ice. So some clouds may be distinguished from snow and ice by brightness temperature. According to tests, it was found that the difference between channel 1 and channel 2 is useful to distinguish clouds and snow-ice, that is, the value of clouds is relative low and the value of snow and ice is relative high. Figure 1a shows the image of channel 2 reflectivity in Beaufort Sea and Alaska in the south in June 22, 2004. Figure 1b shows the corresponding image of the difference of channel 1 and channel 2. In figure 1a, the reflectivity of clouds, snow and ice are all high, so it is impossible to distinguish them by the reflectivity of visible band, but the texture of snow and ice is apparently smoother than that of clouds. Therefore, the next portion will have a detailed analysis of the texture feature of clouds, snow and ice. In figure1b, most clouds are more dark than snow and ice, so the difference between channel 1 reflectivity and channel 2 reflectivity is an important difference between clouds and snow-ice.

A simple discriminant method was designed by the reflectivity and the reflectivity difference between channel 1 and channel 2. The thresholds are set as follows:

$$\text{water}: \begin{cases} 0\% < [CH1 - CH2] \leqslant 10\% \\ CH2 < 20\% \end{cases}$$

$$\text{land}: \begin{cases} [CH1 - CH2] < 0\% \\ CH2 < 50\% \end{cases}$$

$$\text{partial clouds}: \begin{cases} 0\% < [CH1 - CH2] < 8\% \\ CH2 > 25\% \end{cases}$$

CH1 and CH2 are the reflectivity of channel 1 and channel 2, respectively. CH1-CH2 is the difference between the reflectivity of channel 1 and channel 2. By using this threshold discriminant method, most clouds can be distinguished from snow and ice. In the next part, texture feature is used for further distinguishing clouds and snow-ice.

3.2 *Texture feature analysis*

Texture is a concept often used to describe images. Haralick first proposed Grey Level Co-occurrence Matrix (GLCM)[22], which is a widely used texture statistical method. GLCM reflects the synthetic information of direction, intervals, change width of image grey level, and can be used to analysis images' unit and arrange structure. The GLCM method assumed that textural information is characterized by a set of co-occurrence matrices $P(i, j, d, \theta)$, where (i, j) the element is the relative frequency with which two pixels separated at the distance d occur in image. $P(i, j, d, \theta)$ is generally expressed by matrix, so it is called as Grey Level Co-occurrence Matrix. Generally, θ is considered 0°, 45°, 90°, 135° respectively, and then $P(i, j, d, \theta)$ is a symmetry matrix. Haralick defined 14 texture features such as contrast, entropy, inverse difference moment, correlation, angular second moment and so on[23]. The formulas are listed as follows:

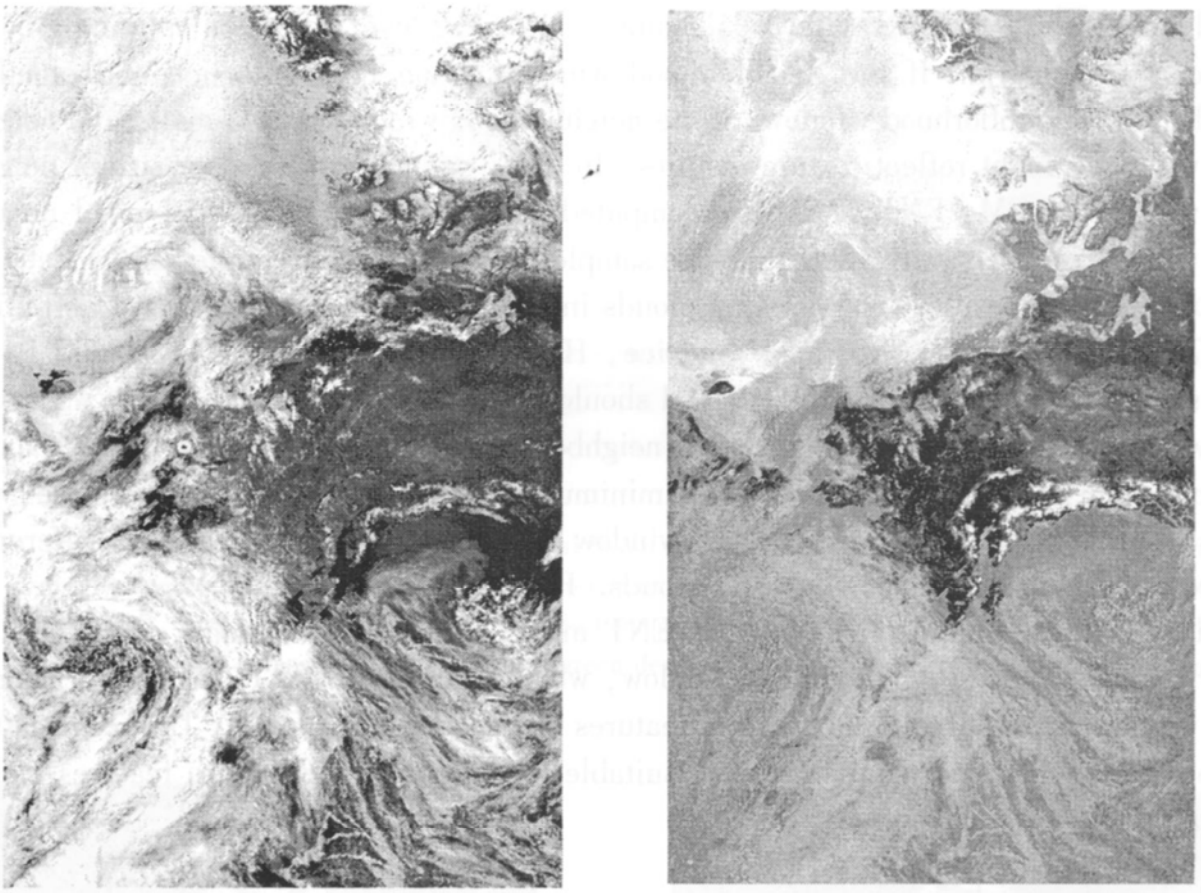

Fig. 1 Comparison of the reflectivity of channel 2 (left) with the difference between reflectivity of channel 1 and reflectivity of channel 2 (right).

Table 1. Texture features compute formula

Texture feature	Formula
Contrast	$CON = \sum_{n=0}^{L-1} n^2 \left\{ \sum_{i=0}^{L-1} \sum_{j=0}^{L-1} \hat{p}(i,j) \right\}$
Entropy	$ENT = \sum_{i=0}^{L-1} \sum_{j=0}^{L-1} \hat{p}(i,j) \log_2 \hat{p}(i,j)$
Inverse difference moment	$HOM = \sum_{i=0}^{L-1} \sum_{j=0}^{L-1} \frac{\hat{p}(i,j)}{1+(i-j)^2}$
Correlation	$COR = \sum_{i=0}^{L-1} \sum_{j=0}^{L-1} \frac{ij\hat{p}(i,j) - u_1 u_2}{\sigma_1^2 \sigma_2^2}$
Angular second moment	$ASM = \sum_{i=0}^{L-1} \sum_{j=0}^{L-1} \hat{p}^2(i,j)$

u_1, u_2, σ_1, σ_2 are defined as

$$u_1 = \sum_{i=0}^{L-1} i \sum_{j=0}^{L-1} \hat{p}(i,j), \quad u_2 = \sum_{j=0}^{L-1} j \sum_{i=0}^{L-1} \hat{p}(i,j)$$

$$\sigma_1^2 = \sum_{i=0}^{L-1} (i-u_1)^2 \sum_{j=0}^{L-1} \hat{p}(i,j), \quad \sigma_2^2 = \sum_{j=0}^{L-1} (j-u_2)^2 \sum_{i=0}^{L-1} \hat{p}(i,j)$$ These texture features are mean value of four direction (0°, 45°, 90°, 135°). In order to reduce computational

complexity, the images' grey level is compressed to 256 level before calculating grey level co-occurrence matrix. If the neighborhood window is too big, snow-ice and clouds are mixed in one neighborhood window; if the neighborhood window is too small, one neighborhood window cannot reflect texture features. In order to choose the proper size of neighborhood window, HOM, ENT, ASM are computed with 3 × 3, 7 × 7, 13 × 13 pixel neighborhood window, respectively. 200 snow-ice samples and 200 clouds samples are selected specially at the boundary of snow-ice and clouds in the images. According to the definition of those texture features, as for snow and ice, HOM should be high, ENT should be low, ASM should be high; as for clouds, HOM should be low, ENT should be high, ASM should be low. Table 2 shows that if 3 × 3 pixel neighborhood window is selected, HOM maximum and minimum, ENT maximum and ASM minimum of snow-ice and clouds are close, which is the result of 3 × 3 pixel neighborhood window is too small to demonstrate the difference of texture features between snow-ice and clouds. If 13 × 13 pixel neighborhood window is selected, HOM maximum, HOM mean, ENT minimum, ASM maximum, ASM mean are closer than 7 × 7 pixel neighborhood window, which is the result of 13 × 13 pixel neighborhood window is too large to mix texture features of snow-ice and clouds. The result is that 7 × 7 pixel neighborhood window is most suitable for analyzing the texture features of snow-ice and clouds.

Table 2 Neighborhood window selection analysis

		3 × 3			7 × 7			13 × 13		
		max	min	mean	max	min	mean	max	min	mean
HOM	Cloud	0.82	0.02	0.35	0.66	0.08	0.39	0.72	0.16	0.43
	Snow-ice	1.0	0.18	0.74	1.0	0.32	0.73	0.96	0.4	0.71
ENT	Cloud	0.82	0.02	0.35	0.66	0.08	0.39	0.72	0.16	0.43
	Snow-ice	1.0	0.18	0.74	1.0	0.32	0.73	0.96	0.4	0.71
ENT	Cloud	2.19	1.0	1.95	3.77	2.33	3.23	4.75	2.46	3.81
	Snow-ice	2.19	0.0	0.89	3.19	0.0	1.38	3.63	0.59	1.89
ASM	Cloud	0.48	0.11	0.15	0.16	0.02	0.05	0.16	0.01	0.04
	Snow-ice	1.0	0.11	0.52	1.0	0.06	0.40	0.75	0.07	0.29

Both channel 1 and 2 are reflectivity images, and they have the same texture features; both channel 3 and 4 are brightness temperature images, and they also have the same texture features. So only the texture features of channel 2 and 3 are computed. In order to reduce compute time and improve discriminant accuracy, texture features are screened by stepwise discriminant analysis. The result is that HOM, ENT, ASM, COR of channel 2 and HOM of channel 3 are most effective texture features to distinguish snow-ice and clouds. Figure 2a shows the ability of spectral features distinguishing snow-ice, clouds, land and water. Figure 2b shows the ability of texture features distinguishing snow-ice from clouds.

4 Classification

Classical Bayes discriminant method is used to distinguish snow-ice from clouds. It is

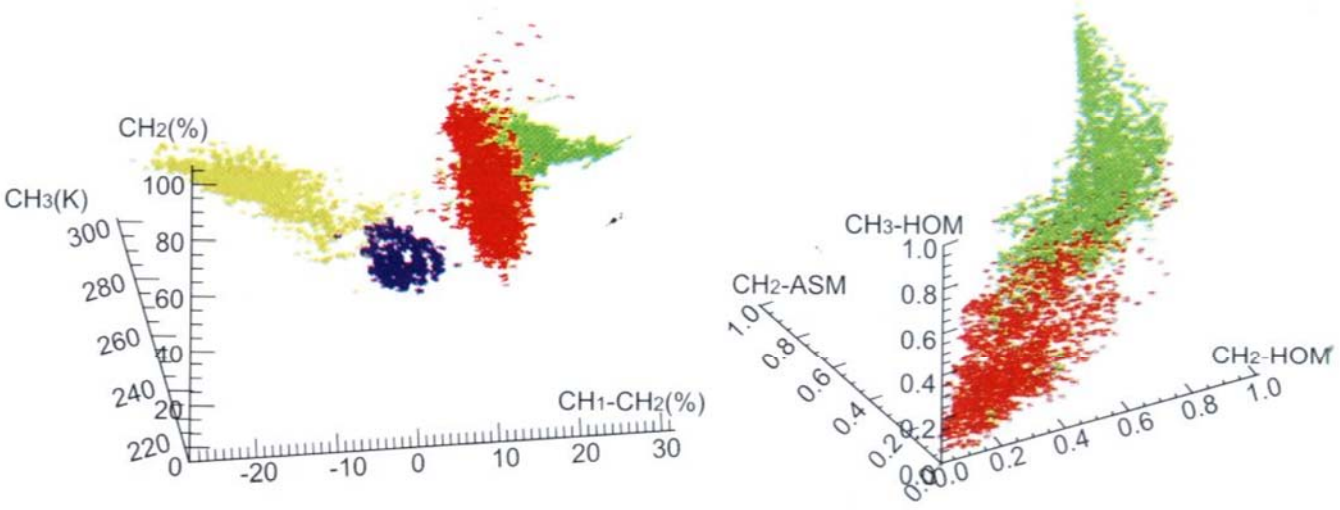

Fig 2 Scatter diagram of various samples' spectral features that include reflectivity in channel 2, brightness temperature in channel 3 and the difference between reflectivity in channel 1 and reflectivity in channel 2, and textural features that include homogeneity of channel 2, angular second moment of channel 2, and homogeneity of channel 3 (green denotes snow-ice, red denotes cloud, blue denotes water, filemot denotes land).

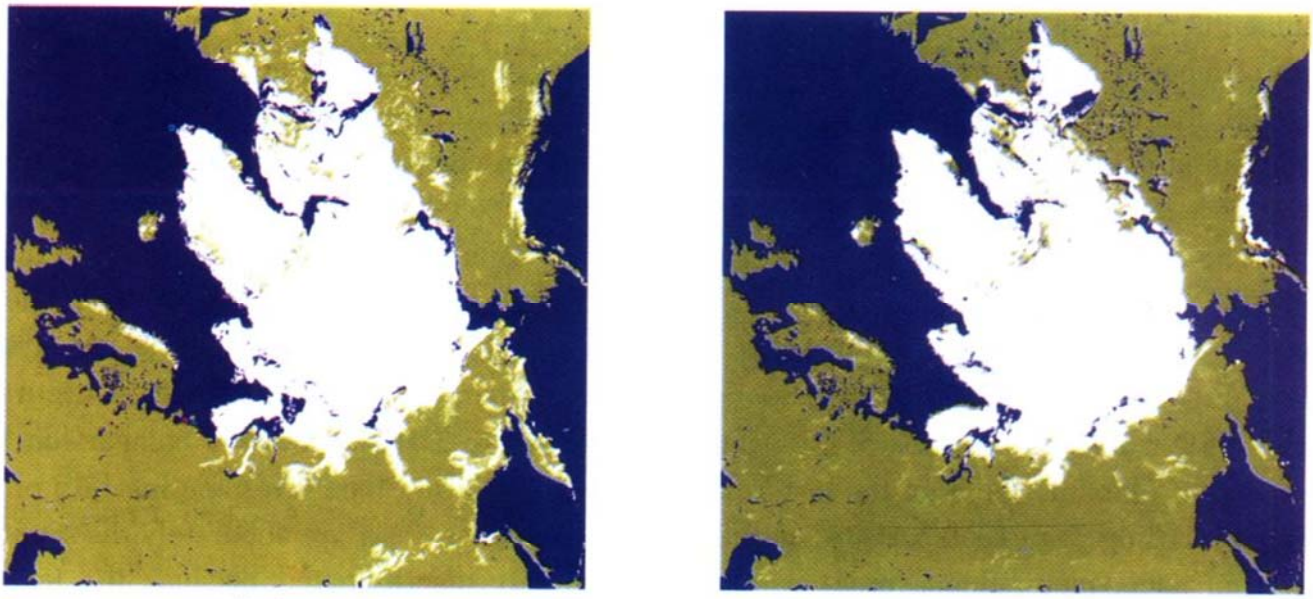

a: IMS product b: discriminant result

Fig 3 Comparison between discriminant result and the product of IMS a IMS product b discriminant result

one of the best classification methods with high accuracy, which is based on Bayes decision-making rules[24]. Its principle is discriminating objects on the premise of a certain degree of knowledge of these objects. Prior probability q_i is set by the proportion of test samples quantity. Assumed that the losses of false judgment c are equal, that is, $c(1|2) = c(2|1)$. $X = \{X_1, X_2, \cdots, X_n\}$, n is the number of samples. G_1 means snow and ice, G_2 means cloud. And they are in p-dimensional normal distribution. The probability density is

$$f_i(x) = (2\pi)^{-\frac{n}{2}} |\sum_i|^{-\frac{1}{2}} \exp\left[-\frac{1}{2}(x-\mu_i)^T \sum_i^{-1}(x-\mu_i)\right], \quad i = 1, 2$$

μ_i is the vector of mean. $\Sigma_i (i = 1, 2)$ is covariance matrix. $|\Sigma_i|$ is determinant of matrix

$\sum_i (i = 1, 2)$. The discriminant formula is

$$\begin{cases} x \in G_1, \text{ if } W^*(x) \geqslant K, \\ x \in G_2, \text{ if } W^*(x) < K, \end{cases}$$

where

$$W^*(x) = -\frac{1}{2} x^T \left(\sum_1^{-1} - \sum_2^{-1} \right) x + \left(\mu_1^T \sum_1^{-1} - \mu_2^T \sum_2^{-1} \right) x$$

$$K = \ln \left| \frac{q_2 c(1/2)}{q_1 c(2/1)} \right| + \frac{1}{2} \ln \left| \frac{|\sum_1|}{|\sum_2|} \right| + \frac{1}{2} \left(\mu_1^T \sum_1^{-1} - \mu_2^T \sum_2^{-1} \right) x$$

$$\mu_1 = x^{\bullet(1)}, \ \mu_2 = x^{\bullet(2)}, \ \sum_1 = S_1, \ \sum_2 = S_2$$

$x^{\bullet(1)}$ and $x^{\bullet(2)}$ are mean value of all features of G_1 and G_2, respectively. S_1 and S_2 are covariance matrix of all features of G_1 and G_2, respectively.

5 Comparison with MS

The United States National Oceanic and Atmospheric Administration/National Environmental Satellite Data, and Information Service (NOAA/NESDIS) has an extensive history of monitoring snow and ice coverage. NOAA began development of the MS in 1995 in order to make a daily snow map feasible. Use MS Daily Northern Hemisphere Snow and Ice Analysis at 4 km resolution to verify the results that are computed by the method described above.

The discriminant result is synthesized by 5 days dsicriminant results, in order to minimize the influence of clouds. As to overlapping areas, data with high solar zenith angle is prior to data with low solar zenith angle. Select the discriminant results of the last 5 days of May, June, July of 2004 and 2005 to verify the discriminant accuracy. The highest accuracy is 90.75%, and the lowest accuracy is 72.14%. Figure 3 shows that the comparison between discriminant results of the last 5 days of June, 2004 and the corresponding MS product. According to the comparison, most snow and ice cover areas are accurately discrimina-

The primary goal of this work is to obtain snow and ice coverage areas by FY-1D MVISR/GDPT. According to the spectral features described above, a simple threshold method can be used to discriminate land, water, and some parts of clouds. Using the difference of textural features between snow-ice and cloud is a feasible method to distinguish snow-ice from clouds with FY-1D/MVISR GDPT data. Select gray level co-occurrence matrix to compute texture features. Stepwise discriminate method is used to filter textural features, and 5 comparative important textural features are selected: homogeneity of channel 2, entropy of channel 2, angular second moment of channel 2, correlation of channel 2 and homogeneity of channel. The suitable neighborhood window size is 7×7.

Classical Bayes discriminant classifier is effective to divide snow-ice from clouds with

selected texture features, but there are some errors for the reason that the prior probability cannot be accurately given. The texture feature of snow is complex, therefore some areas covered by snow, especially mountainous area covered by snow, cannot be accurately identified. In further work, enhancing sample storages of all types and building independent snow sample storage may be useful to improve the discriminating accuracy.

References

[1] IGBP (2001): Towards global sustainability. IGBP Science Series, 4: 27-29.

[2] IPCC (1996): Climate change 1995, The Science of Climate Change. Cambridge: Cambridge University Press, 1996.

[3] IPCC (2001): Climate Change 2001, The Scientific Basis. Cambridge: Cambridge University Press, 2001.

[4] Vinnikov KY, Robock A, Stouffer RJ, Walsh JE *et al.* (1999): Global warming and northern hemisphere sea ice extent. Science, 1999, 286(5446): 1934-1937.

[5] Welch RM, Sengupta SK, Goroch AK (1992): Polar cloud and surface classification using AVHRR imagery: an intercomparison of methods. J Appl Meteor, 31(5): 405-420.

[6] Emery W J, Radebaugh M, Fowler C W, Cavalieri D J, Steffen K A (1991): comparison of sea ice parameters computed from advanced very high resolution radiometer Landsat imagery and from airborne passive microwave radiometer. J Geophys Res., 1991, 96(C2): 22075-22085.

[7] Massom R, Comiso JC (1994): The classification of Arctic sea ice types and the determination of surface temperature using advanced very high resolution radiometer data. J Geophys Res, 99(C3): 5201-5218.

[8] Comiso JC (1983): Sea ice effective microwave emissivities from satellite passive microwave and infrared observations. J Geophys Res, 88(C12): 7686-7704.

[9] Cavalieri D J, Gloersen P, Campbell W J (1984): Determination of sea ice parameters with Nimbus-7 SMMR. J Geophys Res, 89(D4): 5355-5369.

[10] Kwok R, Rignot E, Holt B, Onstott R (1992): Identification of sea ice types in space borne synthetic aperture radar data. J Geophys Res, 97(C2): 2391-2402.

[11] Kwok R, Cunningham GF (1994): Backscatter characteristics of the winter ice cover in the Beaufort Sea. J Geophys Res, 99(C4): 7787-7802.

[12] Swift CT, Fedor LS, Ramseier RO (1985): An algorithm to measure sea ice concentration with microwave radiometers. J Geophys Res, 90(C1): 1087-1099.

[13] Cavalieri D J (1994): A microwave technique for mapping thin sea ice. J Geophys Res, 99(C6): 12561-12572.

[14] Kwok R, Comiso JC, Cunningham GF (1996): Seasonal characteristics of the perennial ice cover of the Beaufort Sea. J Geophys Res, 101(C12): 28417-28439.

[15] Eicken H, Dmitrenko I, Tyshko K *et al.* (2005): Zonation of the Laptev Sea landfast ice cover and its importance in a frozen estuary[J]. Global and Planetary Change, 48(1-3), 55-83.

[16] Belchansky G, Douglas DC (2002): Seasonal comparisons of sea ice concentration estimates derived from SSM/I, OKEAN, and RADARSAT data [J]. Remote Sensing of Environment, 81(1): 67-81.

[17] Liu YJ (2001): Study on the data processing and application of FY-1C satellite [J]. Aerospace Shanghai, 18(2): 74-78.

[18] Kidder SQ, Wu HT (1984): Dramatic contrast between low clouds and snow cover if daytime 3.7μm imagery. Mon Wea Rev., 112(11): 2345-2346.

[19] Robert CA Jr, Philip AD, Carlyle HW (1990): Snow/Cloud Discrimination with Multispectral Satellite Measurements[J]. J Appl Meteor, 29(10): 994-1004.

[20] Stowe LL, McClain EP, Carey R, *et al.* (1991): Global distribution of cloud cover derived from NOAA/AVHRR operational satellite data. Advances in Space Research, 11(3): 51-54.

[21] Meng ZZ, Dong YH (2002): The FY-1D polar orbiting meteorology satellite[J]. Aerospace Shanghai,

19(5): 1-8.

[22] Haralick RM, Shanmugan KS, Dinstein I(1973): Textural feature for image classification. IEEE Trans. Sys. Man. Cybern, SMC-3(6): 610-621.